doi: 10.4149/gpb_2017009

Inhibition of PDE4 by low doses of rolipram induces changes in lipid and protein components of mice heart

Sevgi Türker-Kaya[1], İpek Komsuoğlu Celikyurt[2], Umut Celikyurt[3] and Aygül Kına[1]

[1] *Department of Biology, Faculty of Arts and Sciences, Kocaeli University, 41380, Kocaeli, Turkey*
[2] *Department of Pharmacology, Faculty of Medicine, Kocaeli University, 41380, Kocaeli, Turkey*
[3] *Department of Cardiology, Faculty of Medicine, Kocaeli University, 41380, Kocaeli, Turkey*

Abstract. There is significant increasing interest in phosphodiesterase-4 (PDE4) inhibition in treatment of cardiovascular diseases. Related with this, research has focused on cellular, biochemical, molecular and structural changes in heart tissue induced by PDE4s inhibitors. However, for their clinical applicability additional studies are still needed. Fourier transform infrared spectroscopy offers promising approach to contribute such issue due to its ability in detection the changes in biomolecules. By utilizing this method, we examined the effects of PDE4 inhibition by rolipram at 0.05 mg/kg and 0.1 mg/kg doses on content of lipids and proteins, and fluidity, order and packing of membranes in naive mice heart. In treated groups, there was a significant decrease in unsaturated, saturated lipids, cholesterol esters, fatty acids, phospholipids and triacylgylcerols obtained from CH_2, C=O, olefinic=CH, and COO^- areas, and CH_2/lipid, C=O/lipid, olefinic=CH/lipid, and COO^-/lipid ratios. Additionally, olefinic=CH area and olefinic=CH/lipid ratio may suggest decreased lipid peroxidation, confirmed by thiobarbituric acid assay. Also, a higher degree of membrane order, slight increase in membrane fluidity and differences in membrane packing were obtained. Amide I and II areas and RNA/protein ratios showed that variation in protein content is not correlated with applied concentration. Analysis of amide I mode predicted alterations in secondary structures like an increase in random coils and decrease in alpha-helices. Moreover, all groups were successfully discriminated by cluster analysis. The corresponding results may help to understand the potential effects of PDE4 inhibition by rolipram.

Key words: Rolipram — Heart — FTIR — Lipid — Protein — Membrane order/packing/fluidity

Abbreviations: BHT, buthylatedhydroxytoluene; cAMP, cyclic adenosine 3',5'-monophosphate; DMSO, dimethyl sulfoxide; FT-IR, Fourier transform infrared; IR, infrared light; LPEPs, lipid peroxidation end products; MDA, malondialdehyde; PDE4, phosphodiesterase 4; ROS, reactive oxygen species; TBA, thiobarbituric acid; TCA, trichloroacetic acid.

Introduction

Cyclic adenosine 3',5'-monophosphate (cAMP) is the main second messenger of β-adrenergic receptor signalling inducing phosphorylation of L-type Ca^{2+} channels and ryanodine receptor to increase the amount of intracellular Ca^{2+} necessary for heart contractility (Mika et al. 2012; Eschenhagen 2013). And, proper cardiac function relies on fine-tuning balance between the synthesis and degradation of cAMP (Boularan and Gales 2015).

3',5'-cyclic nucleotide phosphodiesterases (PDEs) regulate the localization, duration, and amplitude of the second messengers (Rao and Xi 2009; Mika et al. 2012; Eschenhagen 2013). Of these, phosphodiesterase-4 (PDE4) enzymes with subtypes of PDEA,B,C,D, are crucial in shaping global cAMP signals in cardiac myocytes in rodents (Verde et al. 1999) and in humans (Mika et

Correspondence to: Sevgi Türker-Kaya, Department of Biology, Kocaeli University, 41380, Kocaeli, Turkey
E-mail: sevgitrkr@gmail.com
sevgi.turker@kocaeli.edu.tr

al. 2012; Molina et al. 2012). Thus, inhibition of PDE4s exhibits hemodynamic and inotropic properties that may be valuable to clinical practice (Goldhaber and Hamilton 2010; Molina et al. 2012; Guglin and Kaufman 2014). Related with this, numerous studies are focused on the mode action of PDE4 inhibitors with their side effects on heart. However, the overall picture of PDE4s inhibition with their inhibitors is still uncertain and additional research is necessary for clinical applicability (Rao and Xi 2009; Mika et al. 2012; Molina et al. 2012; Eschenhagen 2013). To contribute these studies Fourier transform infrared (FT-IR) spectroscopy offers promising approach due to its ability in detection of the changes on content, structure and dynamics of biomolecules in cells and tissues (Derenne et al. 2012; Ozek et al. 2014; Turker-Kaya et al. 2016). It is a rapid technique that does not require any staining nor complicated sample preparation (Derenne et al. 2012; Turker et al. 2014a). Infrared (IR) spectrum of a biological sample represents the sum of various contributions from lipids, proteins, carbohydrates, nucleic acids and all other chemical species (Carmona et al. 2008; Miller et al. 2013; Ozek et al. 2014; Turker et al. 2014a, 2014b). The intensities and/or areas provide quantitative information, peak positions relate to physical states of molecules, and bandwidth gives dynamical information (Severcan et al. 2005; Carmona et al. 2008; Miller et al. 2013; Kumar et al. 2014; Ozek et al. 2014; Turker et al. 2014a, 2014b; Turker-Kaya et al. 2016). As a result, it is possible to monitor global effects of chemicals and conditions on all of the constituents in biological systems (Gasper et al. 2009; Ozek et al. 2014; Turker-Kaya et al. 2016). By taking its advantages FT-IR spectroscopy has been increasingly employed to investigate molecular alterations induced by drugs and even disease' states, which is not easily detectable by morphological methods, in cells and tissues (Amharref et al. 2006; Akkas et al. 2007; Berger et al. 2010; Leskovjan et al. 2010; Cakmak et al. 2011; Bellisola et al. 2012; Bozkurt et al. 2012; Travo et al. 2012; Turker et al. 2014a, 2014b; Turker-Kaya et al. 2016).

There are different types of PDE4 inhibitors that show distinctive selectivity for PDE4 subtypes. For example, ibudilast has been shown to potently inhibit purified human PDE 4A, 4B, 4C and 4D with IC50 values of 54, 65, 239 and 166 nM, respectively (Huang et al. 2006). Cilomilast is ten-fold more selective for PDE4D compared to other PDE4 subtypes (Rennard et al. 2006). On the other hand, roflumilast does not demonstrate any PDE4 subtype selectivity (Hatzelmann and Schudt 2001). Similarly, as being selective inhibitor of all isoenzymes of PDE4s rolipram, a well-characterized PDE4 inhibitor, was developed as an effective antidepressant, and later tested for treating asthma and chronic pulmonary disease (COPD) (McKenna et al. 2006). Although it was hampered due to its gastrointestinal side effects, it has been still used in research investigating potential use of PDE4 inhibition against several pathologies including cardiovascular diseases (Kenk et al. 2010; Leroy et al. 2011; Molina et al. 2012; Fu 2014).

In the current study, we aimed to acquire a general point of view on the effects of PDE4 inhibition by rolipram at low concentrations (0.05 mg/kg and 1.0 mg/kg) on whole naive mice heart. We have evaluated the variations of spectral parameters of control and rolipram-treated groups as also performed in previous studies (Cakmak et al. 2011; Bozkurt et al. 2012; Ozek et al. 2014; Turker-Kaya et al. 2016). We have obtained the relative changes in lipid and proteins content, and membrane lipid packing, membrane fluidity, and membrane order and lipid peroxidation, all of which are very important parameters for proper function of heart. Moreover, by detailed analysis of Amide I mode we also predicted the changes in protein secondary structures. We have successfully discriminated control and treated groups depending on their spectra using cluster analysis (Severcan et al. 2010; Turker et al. 2014b). To the best of our knowledge, such approach based on spectral parameters resulted from PDE4 inhibition by rolipram action on naïve heart has been not reported, previously.

Materials and Method

Animal care and drug treatment

Male inbred BALB/c mice (n = 22) weighing 40 g (Mam Tubitak, Gebze, Kocaeli, Turkey), aged 7 weeks upon arrival the laboratory. The animals (4–5 *per* cage) were kept in the laboratory at 21 ± 1.5°C with 60% relative humidity under a 12 h light/dark cycle (light on at 8.00 p.m.) during 2 weeks before experiments. Tap water and food pellets were available *ad libitum*. All procedures involving animals were in compliance with the European Community Council Directive of 24 November 1986, and ethical approval was granted by the Kocaeli University Ethics Committee (Number: AEK 9/4-2010, Kocaeli, Turkey).

Rolipram were purchased from Sigma Chemical Company (Sigma, St.Louis, MO) and dissolved in saline supplemented with small amounts of dimethyl sulfoxide (DMSO). The drug was freshly prepared before *intraperitoneally* (*i.p.*) administration in a volume of 0.1 ml *per* 10 g body weight. All animals were divided into three groups: control group received vehicle, 0.05 and 0.1 mg/kg doses of rolipram were given to related treated groups for each day during 15 days. At the end of the application procedure the animals were decapitated and whole heart samples were dissected out and kept in –80°C till FT-IR spectroscopic studies.

Sample preparation for FT-IR studies

To eliminate possible biological discrepancy among distinct heart regions, where PDE4 activity is not evenly distributed, we prepared the samples from whole heart tissue. The whole heart samples were dried in a Labconco freeze drier (Labconco FreeZone®, 6 litre Benchtop Freeze Dry System Model 77520) overnight in order to remove the water content. The samples were ground to obtain tissue powder, which were later mixed with dried potassium bromide (KBr) at the ratio of 1/100. The mixture was dried again in the freeze drier for 18 hours to remove all traces of remaining water. And then, in order to obtain same thickness of each pellet same amount of sample was weighted and same pressure ~100 kg/cm^2 (1300 psi) was applied to produce a thin KBr disk of all samples (Elibol-Can et al. 2011; Turker-Kaya et al. 2016).

FT-IR spectroscopic analysis

Infrared spectra were obtained using a Perkin-Elmer Spectrum One FTIR spectrometer (Perkin-Elmer Inc., Norwalk, CT, USA) equipped with a MIR TGS detector. The spectra of samples were recorded in the 4000–400 cm^{-1} region at room temperature. Each interferogram was collected with 100 scans at 4 cm^{-1} resolution. In order to remove the interference of water and carbondioxide effects on IR spectra the spectrum of air and KBr transparent disk was recorded together as background and substracted automatically by using Spectrum One software (Perkin-Elmer).

Even though we performed special care to produce same thickness of each KBr pellet, to minimize intra-sample variability which may be caused by variations in experimental conditions, we scanned three independent pellets prepared by taking separate portions randomly from the same sample. The average spectra of three replicates giving identical spectra represented one animal were used in both detailed data analysis and statistical analysis as same approach performed in previous studies (Akkas et al. 2007; Cakmak et al. 2011; Ozek et al. 2014; Turker et al. 2014b).

Spectrum One software was used to analyse spectral data by following earlier reports (Elibol-Can et al. 2012; Ozek et al. 2014; Turker-Kaya et al. 2016). The band positions were measured using the frequency corresponding to the centre of 80% × height of the peak. The peak area was calculated as related to a linear baseline between two baseline points which involve the maximum peak height. The baseline point was identified according to start and end points of the peak. Later, the corrected area which is the area between the spectrum and the marked baseline within the marker bar limits was found the peak area value of the interested peak. The bandwidth values of specific bands were calculated as the width at 0.80 × height of the signal in terms of cm^{-1}.

Again still considering possible interference due to detectable variability of sample thickness area ratios of some specific IR modes were also evaluated to approximate content changes in biomolecules since we did not apply any biochemical assay to measure content of biomolecules of interest as performed previously (Antoine et al. 2010; Turker-Kaya et al. 2016). For the CH_2/lipid, C=O/lipid, olefinic=CH/lipid, and COO^-/lipid ratios, the areas under the CH_2 asymmetric stretching (2925 cm^{-1}), the C=O stretching (1750 cm^{-1}), the olefinic=CH (3012 cm^{-1}), and the COO^-symmetric (1390 cm^{-1}) modes were divided to the total saturated lipid (the sum of the area under the CH_2 asymmetric and symmetric stretching bands). For RNA/protein ratio, the area under C-N-C stretching (998 cm^{-1}) were divided to the sum of the area under the amide I and II bands.

The same software was also used for smoothing, baseline correction and normalization processes. The spectra were first smoothed with nineteen-point Savitsky-Golay smooth function to remove the noise. And then, baseline correction was applied based on specific points. Normalization was performed with respect to specific bands. It should be worth noting that all these procedures were performed only for visual representation of the differences among the groups. For accurate evaluation of the spectral parameters the original average spectrum from each animal was analyzed.

In order to predict the alterations in protein secondary structure elements, amide I mode was further analyzed by OPUS 5.5 (Bruker Optic, GmbH). Since peak height/area of this mode is very sensitive to changes of fullwidth at half height in second derivative spectra, concentration sensitive changes in the components of this band were monitored by measuring intensity values of its sub bands. The spectral comparisons of amide I band were carried out on vector normalized second derivatives.

Measurement of lipid peroxidation (TBARs assay)

TBAR, well-adopted test, was performed to monitor lipid peroxidation (Severcan et al. 2005; Turker et al. 2014a). The heart samples were homogenized by Teflon glass homogenizer in cold 0.02 M phosphate buffer (pH 7.4) at a concentration of 25% (w/v). The homogenates were diluted to 5% with the phosphate buffer containing 0.25 ml buthylatedhydroxytoluene (BHT), which prevents artificial increase of malonydialdehyde (MDA). Then, the homogenates were incubated for 60 min at 37°C. After the incubation, 2 ml of trichloroacetic acid (TCA) solution (28% w/v in 0.25 N HCl) was added. The samples were centrifuged at low speed and 4 ml of supernatants were mixed with 1 ml of thiobarbituric acid (TBA) (1% w/v in 0.25 N HCl). Subsequently, the samples were kept in boiling water for 30 min to get chromophore development. The samples were cooled to room temperature and the absorbance values were measured at 532 nm.

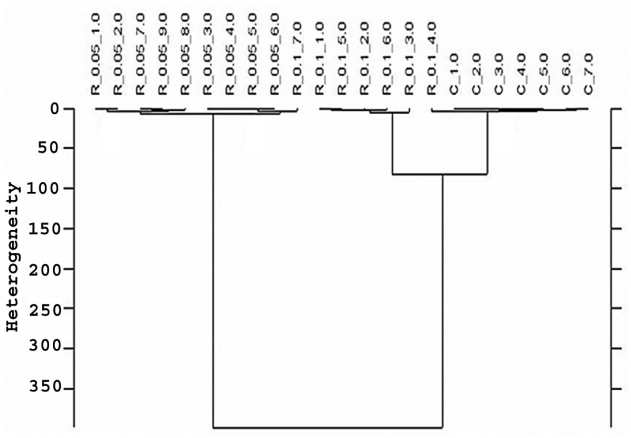

Figure 1. Hierarchial analysis of control, 0.05 mg/kg rolipram, and 0.1 mg/kg rolipram groups for 4000–800 cm^{-1} spectral region.

Cluster analysis

Hierarchical cluster analysis was performed on first derivative spectra using the cluster analysis module of OPUS 5.5 (Bruker Optic, GmbH). It was applied to distinguish between different spectra from control and treated groups using a frequency range between 4000–800 cm^{-1}. As input data for cluster analysis, spectral distances were calculated between pairs of spectra as Pearson's correlation coefficients (Severcan et al. 2010; Turker et al. 2014b). Cluster analysis for separation of control and rolipram treated heart tissues was based on the Euclidean distances. In all cases, Ward's algorithm was used for hierarchical clustering.

Statistical analysis

The results were expressed as mean ± standard deviation. All data were analyzed statistically using non-parametric ANOVA test. p value less than or equal to 0.05 was considered as statistically significant.

Results

Detailed spectral analysis revealed that there are prominent spectral differences in both rolipram-treated groups compared to control ones. Depending on the spectral variations among groups in the region between 4000–800 cm^{-1} cluster analyses was performed to differentiate the groups. And, three distinct clusters were produced with a high accuracy (success rate 9/9 for 0.05 mg/kg, and 6/7 tissues for 0.1 mg/kg). The resultant dendogram is depicted in Figure 1.

In order to easily demonstrate the details of the spectral differences among the groups, the spectra were showed in two separated regions. Figures 2 and 3 show normalized infrared spectra of control, 0.05 mg/kg and 0.1 mg/kg dose of rolipram heart tissues in 3025–2800 cm^{-1} and 1940–800 cm^{-1} region, respectively. In Figure 2, the spectra were normalized with respect to the CH_2 asymmetric stretching band at 2925 cm^{-1}, and in Figure 3, the spectra were normalized with respect to the amide I band at 1645 cm^{-1} for visual demonstration of the spectral variations. The detailed band assignments based upon the literature were given in Table 1. Table 2 represents detailed analysis of spectral modes and results of TBAR's assay for each group.

The changes in the content of lipids have been relatively obtained by analysing the areas of the =CH olefinic (unsaturated lipids), the CH_2 asymmetric and the CH_2 symmetric (saturated lipids), the C=O (triacylglycerols, cholestereol esters and phospholipids) and the COO^- symmetric (fatty acids) as well as olefinic/lipid, CH_2/lipid, C=O/lipid and COO^-/lipid ratios. As shown in Figures 2 and 3 and Table 2, in both treated groups all these areas and area ratios were significantly ($p < 0.05$) reduced.

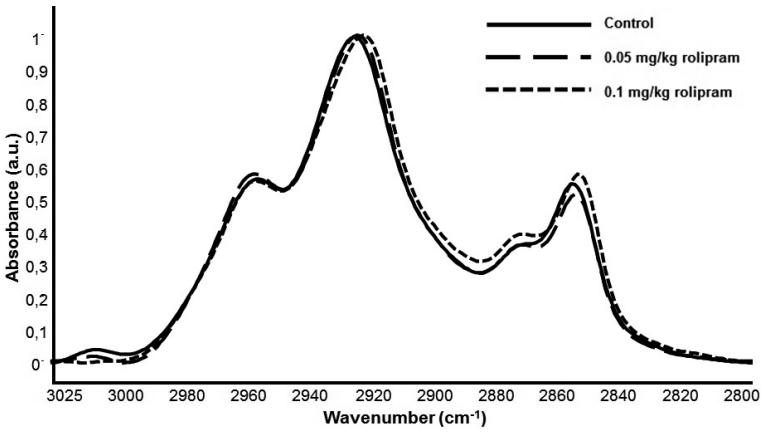

Figure 2. Representative FT-IR spectra of control, 0.05 mg/kg rolipram, and 0.1 mg/kg rolipram groups in the region between 3025–2800 cm^{-1}. The spectra were normalized with respect to the CH_2 asymmetric stretching at 2925 cm^{-1}.

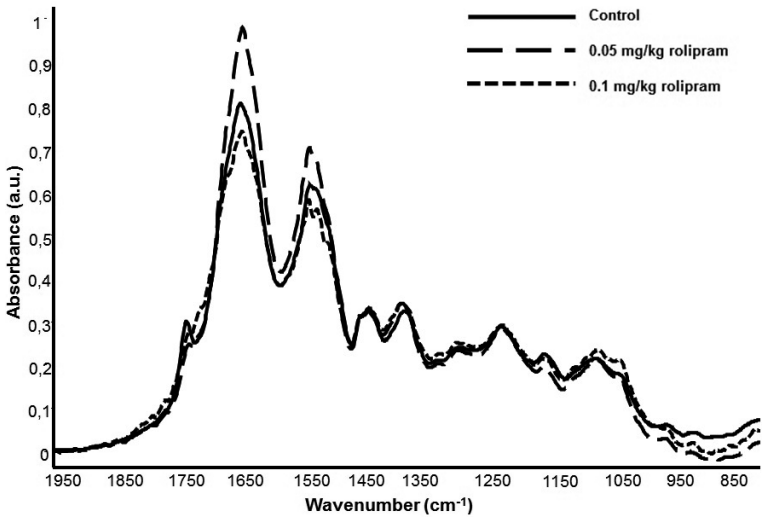

Figure 3. Representative FT-IR spectra of control, 0.05 mg/kg rolipram, and 0.1 mg/kg rolipram groups in the region between 1950–800 cm^{-1}. The spectra were normalized with respect to the amide I at 1645 cm^{-1}.

As demonstrated in Table 2 and Figures 2 and 3, rolipram treatment at both two concentrations led to significant ($p < 0.05$) shiftings to lower values in the CH_2 asymmetric stretching (2925 cm^{-1}), the C=O (1750 cm^{-1}) and the PO^{-}_2 symmetric (1080 cm^{-1}).

Alterations in fluidity of the cell membrane can be determined by probing the bandwidth values of the CH_2 asymmetric stretching mode (Lopez et al. 2001; Ozek et al. 2014; Turker et al. 2014b). This value was slightly increased for 0.05 mg/kg and for 0.1 mg/kg rolipram as illustrated in Figure 2 and Table 2.

The band areas of amide I and amide II modes are directly related with protein content in the system (Elibol-Can et al. 2011; Bozkurt et al. 2012; Turker et al. 2014a). Figure 3 and Table 2 illustrate the areas of these modes significantly ($p < 0.05$) increased for the group of 0.05 mg/kg rolipram but significantly ($p < 0.05$) decreased for 0.1 mg/kg rolipram group.

Amide I mode consists of many overlapping modes that represent different secondary structure elements of proteins such as alpha-helices, beta-turns, turns and random coil (Turker et al. 2014a; Turker-Kaya et al. 2016). Upon analysing of amide I band, the related peaks under amide I were observed in second derivative spectra for control and treated groups (Figure 4). The band at around 1682 cm^{-1} is associated with beta turns, the peak at 1652 cm^{-1} is due to alpha helix, the mode located at 1643 cm^{-1} are assigned to random coil, beta sheet band appears at 1633 cm^{-1} (Turker et al. 2014a; Turker-Kaya et al. 2016). The changes in the intensities of characteristics components of amide I mode were given in Table 3. Compared to control for rolipram groups, a decrement in alpha-helix and beta-sheet ($p < 0.05$) the intensity of beta sheet of amide I band was obtained. More importantly, there is a statistically prominent increment in random coil for both rolipram groups ($p < 0.05$).

The band centred at 990 cm^{-1} is generally assigned to symmetric stretching mode of dianionic phosphate monoester of cellular nucleic acids and ribose-phosphate main chain vibrations of the RNA backbone (Chiriboga

Table 1. General band assignment of heart tissue

Frequency (cm^{-1})	Definition of the Spectral Assignments
3012	Olefinic =CH stretching: unsaturated lipids
2925	CH_2 asymmetric stretching: mainly lipids with little contribution from proteins, carbohydrates and nucleic acids
2852	CH_2 symmetric stretching: mainly lipid with the little contribution from proteins, carbohydrates and nucleic acids
1750	Saturated ester C=O stretch: phospholipids, cholesterol esters, triglycerides
1645	Amide I (protein C=O stretch): proteins
1547	Amide II (C=N and N-H stretching): proteins
1450	COO^{-} symmetric stretching: fatty acids
1080	PO_2^{-} symmetric stretching: phospholipids and nucleic acids
976	C^{+}-N-C stretching: nucleic acids, ribose phosphate main chain vibrations of RNA

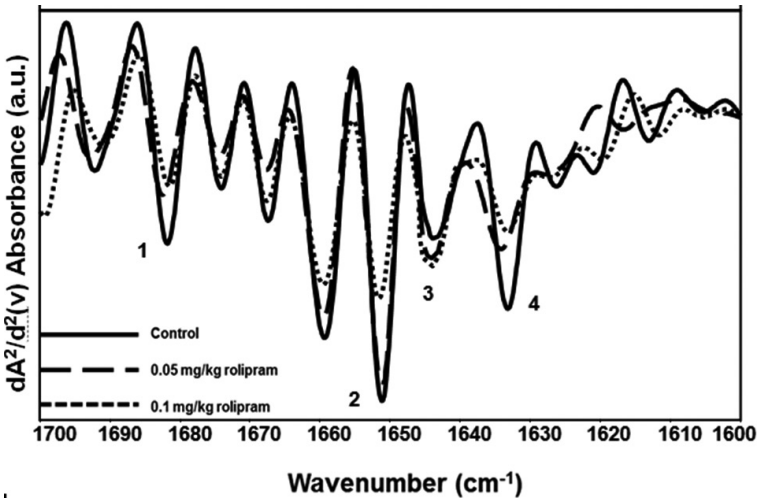

Figure 4. Representative the second derivative spectra of amide I band for control, 0.05 mg/kg rolipram, and 0.1 mg/kg rolipram groups in the region between 1700–1600 cm^{-1}. Vector normalization was done in the 1700–1600 cm^{-1} region. Absorption maxima appear as minima in the second derivatives. The numbered peaks are attributed to: 1, beta turn; 2, alpha helix; 3, random coil; 4, beta sheet.

et al. 2000; Banyay et al. 2003; Ozek et al. 2014). There was a significant ($p < 0.05$) decrease in the area of this band and RNA/protein for both treated groups, indicating a decrease in the nucleic acid, especially RNA content in heart tissue.

Discussion

Whole heart tissue contains various components like cardiac myocytes, cardiac fibrocytes, endothelial cells and extracellular matrix. In such complexity FT-IR spectroscopy lacks

Table 2. The frequency, band area and area ratio values of FTIR bands and MDA levels for control, 0.05 mg/kg and 0.1 mg/kg rolipram groups of heart tissue

	Control	Rolipram	
		0.05 mg/kg	0.1 mg/kg
Frequency			
CH_2 asym	2924.09 ± 0.07	2922.14 ± 0.28*	2921.88 ± 0.44*
C=O	1753.10 ± 0.89	1750.62 ± 1.30*	1750.09 ± 0.91*
PO^-_2 sym	1080.92 ± 0.58	1077.99 ± 1.63*	1076.81 ± 1.12*
Band area			
olefinic	1.78 ± 0.11	1.09 ± 0.07*	0.34 ± 0.09**
CH_2 asym	13.59 ± 0.76	12.68 ± 0.14*	11.27 ± 0.68*
C=O	2.91 ± 0.03	1.07 ± 0.08*	0.90 ± 0.05*
amide I	25.46 ± 0.78	28.51 ± 0.49*	20.09 ± 1.36*
amide II	12.27 ± 1.43	14.70 ± 1.41*	10.05 ± 0.83*
COO^-	3.90 ± 0.06	3.11 ± 0.17*	3.22 ± 0.34*
RNA	4.78 ± 0.67	3.87 ± 0.39*	3.79 ± 0.86*
Band area ratio values			
olefinic/lipid	0.08 ± 0.002	0.05 ± 0.009*	0.02 ± 0.004*
CH_2/lipid	0.61 ± 0.009	0.58 ± 0.007*	0.57 ± 0.006*
C=O/lipid	0.13 ± 0.008	0.05 ± 0.006*	0.04 ± 0.001*
COO^-/lipid	0.17 ± 0.002	0.14 ± 0.002*	0.15 ± 0.003*
RNA/protein	0.12 ± 0.007	0.09 ± 0.008*	0.10 ± 0.005*
Bandwidth			
CH_2 asym	8.44 ± 0.13	8.65 ± 0.16	8.87 ± 0.95
TBARs assay			
MDA (nmol/g)	39.44 ± 2.27	30.05 ± 1.88*	31.54 ± 2.90*

The values are the mean ± SD for each sample. The degree of significance was denoted as * $p < 0.05$.

Table 3. The changes in value of protein secondary structure estimation by second derivative for control, 0.05 mg/kg and 0.1 mg/kg rolipram groups of heart tissue

	Control	Rolipram	
		0.05 mg/kg	0.1 mg/kg
1-Beta turn	–0.0022 ± 0.0004	–0.0019 ± 0.0002*	–0.0018 ± 0.0003*
2-Alpha helix	–0.0049 ± 0.0002	–0.0045 ± 0.0006*	–0.0043 ± 0.0007*
3-Random coil	–0.0021 ± 0.0005	–0.0024 ± 0.0009*	–0.0025 ± 0.0001*
4-Beta sheet	–0.0036 ± 0.0007	–0.0026 ± 0.0004	–0.0023 ± 0.0006*

The values are the mean ± SD for each sample. The degree of significance was denoted as * $p < 0.05$.

providing information about each specific component. But, due to Conne advantage it facilitates the vibrations of functional groups present in biomolecules to represent a variety of different modes appeared at distinct wavenumber values in an FT-IR spectrum. This enables separation of the peaks to be analysed even in weak absorption modes (Gasper et al. 2009; Leskovjan et al. 2010; Elibol-Can et al. 2011; Turker et al. 2014b).

In biological samples although FT-IR spectroscopy gives global information about biomolecules rather than specific ones, it is possible to detect saturated lipids, unsaturated lipids, cholesterol ester, triglycerides, proteins, nucleic acids and carbohydrates, as overall. Therefrom, the current study was conducted to obtain general perspective about the effects of PDE4 inhibition by rolipram on naïve whole mice heart by monitoring the variations in the frequencies, bandwidths and peak areas of the vibrational modes. The alterations in the spectral parameters between the control and treated groups were modest, but they were consistent and statistically significant with marginal standard deviations, as similarly reported (Cakmak et al. 2011; Ozek et al. 2014; Turker-Kaya et al. 2016). Since there are significant changes among control and treated groups, cluster analysis successfully discriminated the spectra. In other words, this analysis revealed that low doses of rolipram administration give rise to important changes in FTIR spectra which can be effectively determined by its application as illustrated in Figure 1.

As one of the disadvantages of FT-IR spectroscopy, it lacks providing quantitative information. But, according to Beer–Lambert law, the intensity and/or, more accurately, the area of absorption bands offer relative information for the content of corresponding functional groups within complex systems (Berger et al. 2010; Leskovjan et al. 2010). This has been previously confirmed by biochemical assays for lipid peroxidation products (LEPs) (Severcan et al. 2005; Leskovjan et al. 2012; Turker et al. 2014a), proteins (Bozkurt et al. 2012) and lipids (Derenne et al. 2012). By utilizing this, in the current study, we have evaluated areas and area ratios of lipid and protein modes to approximate the changes in the content of these molecules without need of biochemical assays.

Lipid molecules are important regulators of cardiac function through their role in membrane phospholipids, as signalling molecules and ligands for nuclear receptors, and as the predominant oxidative substrate for cardiac mitochondria. Regarding this, the effects of PDE inhibitors on such molecules may have prominent importance related to proper heart function. It has been reported that the action of PDE inhibitors increase cAMP level, and thereby raise lipolysis in adipocytes (Chaves et al. 2011). This event may cause deleterious consequences in some pathological conditions such as diabetes mellitus and obesity (Perilli et al. 2013; Arner et al. 2014). Therefore, such inhibitors can be expected to produce some effects on lipid metabolism which could be a potential risk factor for clinical adverse effect in heart. Considering the administration of rolipram to stimulate lipolysis in brown fat tissue (Kraynik et al. 2013) we have approximated the changes in content of lipid components like unsaturated, saturated lipids, cholesterol esters, fatty acids, phospholipids and triacylglycerols. According to the obtained results from the areas of the =CH olefinic, the CH_2 asymmetric, the CH_2 symmetric, the C=O, and the COO^- symmetric stretching together with olefinic/lipid, CH_2/lipid, C=O/lipid and COO^-/lipid ratios, rolipram action has lowering effect on the content of heart lipids. Such decrement in fatty acids, cholesterol esters and triacylglycerols might reveal utilization of these molecules for ATP generation induced by PDE4 inhibition, which might be related with cAMP increasing effect on mitochondrial function and cardiac contractility (Kajimoto et al. 1997; Arner et al. 2014). On the other hand, as another types of lipids, phospholipids have not only pivotal impact on membrane properties but also involve in specific signalling functions necessary for cells to respond to external stimuli. For that reason, membrane phospholipid homeostasis is very important for heart. Related with this, the found decrement in phospholipids together with saturated lipids in the current study has importance for this and shows shortened chain lengths (Turker et al. 2014b). Moreover, such outcome may be reflective of differences in phospholipid signalling that may contribute to the progression of impaired heart function. In sum, it should be noting that the effects of rolipram

on lipid profile in the blood should be evaluated including levels of cholesterol like low and high density lipoprotein. And, further studies are required to confirm the effects of rolipram on lipid content by measuring lipoprotein lipase activity.

Heart tissue relies on oxidative pathway to utilize fuels, and has high content of mitochondria where reactive oxygen species (ROS) are produced (Armstrong and Ianuzzo 1977; Leary et al. 2003). These molecules readily attack lipids and lipid peroxidation occurs, and LEPs are released into extra and intracellular site of cell (Cakmak et al. 2011; Turker et al. 2014a). Therefore, the detection of LEPs may provide information about not only pathogenesis of any condition but also antioxidant capacity of an agent in tissues including heart, also shown by reports in the literature (Battisti et al. 2008; Ramana et al. 2014). In the current study, we have investigated whether PDE4 inhibition by rolipram stimulates lipid peroxidation in heart, or not. Normally, when lipid peroxidation takes place, an increase in olefinic mode area and olefinic/lipid ratio due to LEPs is observed as reported earlier (Turker et al. 2014a). Moreover, when malondialdehyde (MDA), one of the LEPs, is produced, the increment in the C=O mode and C=O/lipid ratio may be also observed (Cakmak et al. 2011). As shown in Figures 2 and 3 and Table 2, significant decreases in areas of the olefinic and C=O mode and olefinic/lipid and C=O/lipid ratios may show low degree of lipid peroxidation, also confirmed by decreased MDA levels. Here, it should be pointed out that both used concentrations of rolipram (0.05 and 0.1 mg/kg) decreased the content of MDA to approximately the same level. It is very well known that the production of MDA occurs by utilization of unsaturated lipids. As we found that 0.1 mg/kg rolipram has more decreasing effect on the content of unsaturated lipids as obtained from reduced area of olefinic mode at 3012 cm^{-1}. This may result in less MDA level produced than expected. The decrement in LEPs might be resulted from intracellular cAMP level, which can suppress the burst of ROS generation (Azadbar et al. 2009). Hence, this finding which showed decreasing effect of rolipram action on lipid peroxidation level in heart also extends the previous reports performed in different tissues (Rezvanfar et al. 2010; Jindal et al. 2015).

Cardiac action potential is critically dependent on membrane compartments which are proteins and lipids. For that reason, the determination of PDE4 inhibition-stimulated changes on membranes has great importance in understanding the effects of this phenomenon on the proper function of heart. So, we have focused on membrane structure, fully mediated through physical properties of fatty acids, polar head groups of lipids, as well as lipid order, lipid fluidity and content of membrane components However, it should be also mentioning that, our sample contains all membranous structures within heart tissue such as sarcolemma, plasma membrane, sarcoplasmic reticulum, and nuclear membrane. Since our preparation contains all membrane compartments, membrane related parameters might reflect the differences in all membrane systems in heart from control and rolipram groups from a general perspective.

The found decline in the content of phospholipids which also show altered lipid composition further affects the organization and packing of lipids (Marsh 1990; Akkas et al. 2007; Turker et al. 2014b). In order to get information about lipid packing parameter we have analyzed the frequency changes of the CH_2 asymmetric, the C=O and the PO_2 symmetric, which reveal the physical state of fatty acyl chains and head groups of membrane phospholipids. The CH_2 stretching vibrations depend on the degree of conformational disorder; hence they can be used to monitor trans/gauche isomerization in the system (Amharref et al. 2006; Ozek et al. 2014; Turker et al. 2014b). The significant shifting to lower values in the CH_2 asymmetric mode may represent an increment in the order of the system, which presents an increase in the number of trans conformers resulting in more rigid membranes (Curatolo, 1987; Akkas et al. 2007; Elibol-Can et al. 2011; Turker-Kaya et al. 2016). Additionally, significantly lowered wavenumber values of the C=O and the PO_2 symmetric bands may imply an increase in the hydration state of the glycerol backbone near the hydrophilic part and polar head group of the membrane lipids. The hydrogen bonding might be between water molecules and the oxygen molecules of both carbonyl and phosphate groups of phospholipids (Akkas et al. 2007; Carmona et al. 2008; Turker et al. 2014b). The variations in physical state of membrane phospholipids may further affect their interaction with hydrophobic and hydrophilic residues of membrane proteins (Turker et al. 2014b). Furthermore, such outcome may have an effect on the functions of glycolipids and glycoproteins which may operate as cell receptors and be responsible for cell signalling (Saberwall and Nagaraj 1994). All of these structural changes in membranes may alter the activity of membrane proteins.

Lipid organization and composition predominantly determine membrane fluidity, which is important for a number of activities including membrane transport, enzyme activity, chemical secretion, and receptor binding and stimulation (Marsh 1990; Antoine et al. 2010). The found slight increment in the bandwidth value of CH_2 asymmetric stretching mode indicates minor effect of PDE4 inhibition by rolipram on fluidity of heart tissue membranes (Akkas et al. 2007; Elibol-Can et al. 2011; Turker et al. 2014b). This might be resulted from a decrease in low content of cholesterol obtained from lower area of C=O and C=O/lipid ratio.

An interesting finding is that applied concentrations of rolipram are not correlated with the changes in protein content obtained from a significant increase for 0.05 mg/kg but decrease for 0.1 mg/kg rolipram in amide I and amide II mode areas, respectively. This may not be contributed to syn-

thesis of some proteins since there was a significant decrease in RNA content with increasing concentration (Chiriboga et al. 2000; Banyay et al. 2003; Bozkurt et al. 2012). On the other hand, it has been reported in the literature that increasing concentration rolipram leads to reduction in muscle protein degradation (Lira et al. 2011). An increase in amide I band area for 0.05 mg/kg might be related with this. However, amide I results indicated that besides reducing proteolysis rolipram has also effects on protein profile of whole heart that is non-linearly related with doses. In order to bring conclusion about rolipram action effects on cardiac proteins content the more extensive experimental design studying larger range of concentrations with even isolated proteins would be beneficial.

Since amide I and amide II profiles also depend on the protein structural composition, the changes in areas and amide I/amide II ratio may suggest that there are some alterations in the structures of proteins (Turker et al. 2014b). Moreover, in recent medical research it has been shown that, compared with the normal tissue, the diseased tissue shows a change in protein secondary structure and ratio of amide I to amide II (Szczerbowska-Boruchowska et al. 2007). In order to better estimate the alterations in protein structure amide I mode was further analyzed as performed in earlier studies (Akkas et al. 2007; Turker et al. 2014b; Turker-Kaya et al. 2016). The results of this study showing significant increase in random coils but decrease in alpha helix and beta sheet structures ($p < 0.05$) might reveal structural change in proteins for rolipram groups. Such changes give information data about protein functions since there is strict relation with their functions and structures. Taking this into consideration, our findings, particularly increase in random coils, reveal denaturation leading to dysfunction of proteins for rolipram groups (Akkas et al. 2007; Turker et al. 2014b; Turker-Kaya et al. 2016). This finding is obviously valuable data since heart muscle contraction is brought about by the interaction of multiple proteins in subcellular structures such as actin, myosin, tropomyosin and troponins. Additionally, again, our preparation contains all membrane compartments, these parameters may be also attributed to the differences in all membrane proteins in heart from control and rolipram groups from a general perspective. For example, a decrease in alpha-helices and beta-sheet structures might suggest that there are changes in membrane lipids between these molecules. This further means that membrane spanning domains of these proteins are then conformationally altered to stabilize membrane curvature (Turker et al. 2014b). All these changes may probably have importance for the regulation of protein functions in heart during PDE4 inhibition. As suggested by Kitsis et al. (1996) such abnormalities in these molecules, major structural and functional components of heart tissue have been postulated to be the cause of contractile dysfunction. These include further cell death and cellular dysfunctions involving contractile proteins, sarcolemma (including associated receptors and channels), sarcoplasmic reticulum and other components of the excitation-contraction coupling apparatus, mitochondria and associated anabolic proteins and various signal transductions. Similarly, it has been reported that unfolded protein response system designed to shut down protein synthesis regulates cardiac sodium current in systolic human heart failure (Gao et al. 2012).

Conclusion

The present study investigated the effects of PDE4 inhibition by rolipram with low two different doses (0.05 and 0.1 mg/kg) in mice heart by FT-IR spectroscopy at molecular level. Detail spectral analysis revealed that rolipram action caused significant changes in the macromolecular content, structure and function in heart tissue. The data indicated differences in membrane packing and a significant decrease in lipid, RNA content, lipid peroxidation but an increase in membrane fluidity and membrane order. Additionally, the change in protein content was found not to be in line with applied concentrations of rolipram. An altered structural profile for proteins was predicted with an increase in random coil whereas a decrease in beta sheet and alpha-helices in both treatment groups.

Depending on these spectral variations control and treated groups could be successfully discriminated by cluster analysis. All these monitored parameters are very important for structure of heart tissue and any change in any of these may further affect its proper functions. For example, alterations in lipids can be observed in myocardial infarction, cardiac arrhythmia and heart failure (Mandel 1995; Moe and Wong 2010; Bui 2011; Harvey and Leinwand 2011; Nordestgaard 2014). Furthermore, the formation of free radicals which further leads to decrease in unsaturated lipids has prominent roles in cardiovascular disease, particularly, atherosclerosis and the associated adverse complications (Smyth et al. 2009; Thomas and Hazen 2010). Moreover, modification in membrane structure in the heart muscle can affect various functions of the membranes by affecting membrane-bound enzymes and receptors directly or indirectly by change in fluidity or permeability of the membranes (Holman 1964; Gudbjarnason and Oskarsdottir 1977). Together with such membrane-related alterations changes in protein structures, it may also cause cardiovascular diseases such as contractile dysfunctions, cardiac amyloidosis, cardiomyopathy and arrhythmia (Mandel 1995; Moe and Wong 2010). For that reason, the findings of the current study can provide a basis for the research on PDE4 inhibition by low doses rolipram, a well-characterized PDE4 inhibitor, and for development of new PDE4 inhibitors.

However, in order to clarify the effects of PDE4 inhibition on heart tissue additional studies including comparison of different PDE4 inhibitors on different animal models of heart failure and arrhythmias should be performed.

Acknowledgement. This study is supported by Scientific Research Foundation (BAP) Kocaeli Universiy Turkey (AEK-9/4-2010).

Conflict of interest. We wish to confirm that there are no known conflicts of interest associated with this publication and there has been no significant financial support for this work that could have influenced its outcome.

References

Akkas SB, Inci S, Zorlu F, Severcan F (2007): Melatonin affects the order, dynamics and hydration of brain membrane lipids. J. Mol. Struct. **834–836,** 207–215 https://doi.org/10.1016/j.molstruc.2006.12.018

Amharref N, Beljebbar A, Dukic S, Venteo L, Schneider L, Pluot M, Vistelle R (2006): Brain tissue characterisation by infrared imaging in a rat glioma model. Biochim. Biophys. Acta **1758,** 892–899 https://doi.org/10.1016/j.bbamem.2006.05.003

Antoine KM, Mortazavi S, Miller AD, Miller LM (2010): Chemical differences are observed in childrens' versus adults' fingerprints as a function of time. J. Forensic. Sci. **55,** 513–518 https://doi.org/10.1111/j.1556-4029.2009.01262.x

Armstrong RB, Ianuzzo CD (1977): Compensatory hypertrophy of skeletal muscle fibers in streptozotocin-diabetic rats. Cell Tiss. Res. **181,** 255–266 https://doi.org/10.1007/BF00219985

Arner P, Langin D (2014): Lipolysis in lipid turnover, cancer cachexia, and obesity-induced insulin resistance. Trends Endocrinol. Metab. **25,** 255–262 https://doi.org/10.1016/j.tem.2014.03.002

Azadbar M, Ranjbar A, Hosseini-Tabatabaei A, Golestani A, Baeeri M, Sharifzadeh M (2009): Interaction of phosphodiesterase 5 inhibitor with malathion on rat brain mitochondrial-bound hexokinase activity. Pestic. Biochem. Physiol. **95,** 121–125 https://doi.org/10.1016/j.pestbp.2009.08.001

Banyay M, Sarkar M (2003): A library of IR bands of nucleic acids in solution. Biophys. Chem. **104,** 477–488 https://doi.org/10.1016/S0301-4622(03)00035-8

Battisti V, Maders LD, Bagatini M D, Santos KF (2008): Measurement of oxidative stress and antioxidant status in acute lymphoblastic leukemia patients. Clin. Biochem. **41,** 511–518 https://doi.org/10.1016/j.clinbiochem.2008.01.027

Bellisola G, Sorio C (2012): Infrared spectroscopy and microscopy in cancer research and diagnosis. Am. J. Cancer Res. **2,** 1–21

Berger G, Gasper R, Lamoral-Theys D, Wellner A, Gelbcke R, Gust J (2010): Fourier Transform Infrared (FTIR) spectroscopy to monitor the cellular impact of newly synthesized platinum derivatives. Int. J. Oncol. **37,** 679–686

Boularan C, Gales C (2015): Cardiac cAMP: production, hydrolysis, modulation and detection. Front. Pharmacol. **6,** 203–207 https://doi.org/10.3389/fphar.2015.00203

Bozkurt O, Bayari S. H, Severcan M, Krafft C, Popp J, Severcan F (2012): Structural alterations in rat liver proteins due to streptozotocin-induced diabetes and the recovery effect of selenium: Fourier transform infrared microspectroscopy and neural network study **17,** 076023

Bui AL, Horwich TB, Fonarow GC (2011): Epidemiology and risk profile of heart failure. Nature Rev. Cardio. **8,** 30–41 https://doi.org/10.1038/nrcardio.2010.165

Cakmak G, Zorlu F, Severcan M, Severcan F (2011): Screening of protective effect of amifostine on radiation-induced structural and functional variations in rat liver microsomal membranes by FT-IR spectroscopy. Anal. Chem. **83,** 2438–2444 https://doi.org/10.1021/ac102043p

Carmona P, Rodríguez-Casado A, Alvarez I (2008): FTIR microspectroscopic analysis of the effects of certain drugs on oxidative stress and brain protein structure. Biopol. **89,** 548–554 https://doi.org/10.1002/bip.20944

Chaves VE, Frasson D, Kawashita NH (2011): Several agents and pathways regulate lipolysis in adipocytes. Biochimie **93,** 1631–1640 https://doi.org/10.1016/j.biochi.2011.05.018

Chiriboga L, Yee H, Diem M (2000): Infrared spectroscopy of human cells and tissues. Part VI: A comparative study of histopathology and infrared microspectroscopy of normal, cirrhotic, and cancerous liver tissue. Appl. Spectrosc. **54,** 1–8 https://doi.org/10.1366/0003702001948204

Curatolo W (1987): Glycolipid function. Biochim. Biophys. Acta **906,** 137–160 https://doi.org/10.1016/0304-4157(87)90009-8

Derenne A, Hemelryck V, Lamoral-Theys D, Kiss R, Goormaghtigh E (2012): FTIR spectroscopy: a new valuable tool to classify the effects of polyphenolic compunds on cancer cells. Biochim. Biophys. Acta **1832,** 46–56 https://doi.org/10.1016/j.bbadis.2012.10.010

Elibol-Can B, Jakubowska-Dogru E, Severcan M, Severcan F (2011): The effects of short-term chronic ethanol intoxication and ethanol withdrawal on the molecular composition of the rat hippocampus by FT-IR spectroscopy. Alcohol Clin. Exp. Res. **35,** 2050–2062 https://doi.org/10.1111/j.1530-0277.2011.01556.x

Eschenhagen T (2013): PDE4 in the human heart - major player or little helper? Br. J. Pharmacol. **169,** 524–527 https://doi.org/10.1111/bph.12168

Fu Q (2014): A long lasting β1 adrenergic receptor stimulation of cAMP/protein kinase A (PKA) signal in cardiac myocytes. J. Biol. Chem. **10,** 14771–14781 https://doi.org/10.1074/jbc.M113.542589

Gao G, Xie A, Zhang J, Herman M, Liu M (2013): Unfolded protein response regulates cardiac sodium current in systolic human heart failure. Circ. Arrhythm. Electrophysiol. **6,** 1018–1024 https://doi.org/10.1161/CIRCEP.113.000274

Gasper R, Dewelle J, Kiss R, Mijatovic T, Goormaghtigh E (2009): IR spectroscopy as a new tool for evidencing antitumor drug signatures. Biochim. Biophys. Acta **1788,** 1263–1270 https://doi.org/10.1016/j.bbamem.2009.02.016

Goldhaber J, Hamilton M (2010): Role of inotropic agents in the treatment of heart failure. Circulation **121,** 1655–1660 https://doi.org/10.1161/CIRCULATIONAHA.109.899294

Gudbjarnason S, Oskarsdottir G (1977): Modification of fatty acid composition of rat heart lipids by feeding cod liver oil. Biochim. Biophys. Acta. **487,** 10–15
https://doi.org/10.1016/0005-2760(77)90039-X

Guglin M, Kaufman M (2014): Inotropes do not increase mortality in advanced heart failure. Int. J. Gen. Med. **7,** 237–251
https://doi.org/10.2147/IJGM.S62549

Harvey PA, Leinwand LA (2011): The cell biology of disease: cellular mechanisms of cardiomyopathy. J. Cell Biol. **194,** 355–365
https://doi.org/10.1083/jcb.201101100

Hatzelmann A, Schudt C (2001): Anti-infl ammatory and immunomodulatory potential of the novel PDE4 inhibitor rofl umilast in vitro. J. Pharmacol. Exp. Ther. **1,** 267–279

Holman R. T. (1964): Nutritional and metabolic interrelationships between fatty acids. Fed. Proc. **23,** 1062–1067

Huang Z, Liu S, Zhang L, Salem M, Greig GM, Chan CC, Natsumeda Y, Noguchi K (2006): Preferential inhibition of human phosphodiesterase 4 by ibudilast. Life Sci. **78,** 2663–2668
https://doi.org/10.1016/j.lfs.2005.10.026

Jindal A, Manesh R, Bhatt S (2015): Type 4 phosphodiesterase enzyme inhibitor, rolipram rescues behavioral deficits in olfactory bulbectomy models of depression: Involvement of hypothalamic-pituitary-adrenal axis, cAMP signaling aspects and antioxidant defense system. Pharmacol. Biochem. Behav. **132,** 20–32
https://doi.org/10.1016/j.pbb.2015.02.017

Kajimoto K, Hagiwara N, Kasanuki H, Hosoda S (1997): Contribution of phosphodiesterase isozymes to the regulation of the L-type calcium current in human cardiac myocytes. Br. J. Pharmacol. **121,** 1549–1556
https://doi.org/10.1038/sj.bjp.0701297

Kenk M, Thackeray JT, Chow BJ (2010). Alterations of pre- and postsynaptic :noradrenergic signaling in a rat model of adriamycin-induced cardiotoxicity. J. Nucl. Cardiol. **17,** 254–263
https://doi.org/10.1007/s12350-009-9190-x

Kitsis MD, Scheuer J (1996): Functional significance of alterations in cardiac contractile protein isoforms. Clin. Cardiol. **19,** 9–18
https://doi.org/10.1002/clc.4960190105

Kraynik SM, Miyaoka RS, Beavo JA (2013): PDE3 and PDE4 Isozyme-selective inhibitors are both required for synergistic activation of brown adipose tissue. Mol. Pharmacol. **83,** 1155–1165
https://doi.org/10.1124/mol.112.084145

Kumar S, Reena S, Chaudhary S (2014): Vibrational studies of different human body disorders using FTIR spectroscopy. OJAppS **4,** 103–129
https://doi.org/10.4236/ojapps.2014.43012

Leary SC, Lyons CN, Rosenberger AG, Ballantyne JS, Stillman J, Moyes CD (2003): Fiber-type differences in muscle mitochondrial profiles. Am. J. Physiol. Regul. Integr. Comp. Physiol. **285,** 817–826
https://doi.org/10.1152/ajpregu.00058.2003

Leroy J, Fischmeister R, Vandecasteele G (2011): Phosphodiesterase 4B in the cardiac L-type Ca2+ channel complex regulates Ca2+ current and protects against ventricular arrhythmias in mice. J. Clin. Invest. **121,** 2651–2661
https://doi.org/10.1172/JCI44747

Leskovjan A, Kretlow A, Miller L (2010): Fourier transform infrared imaging shows reduced unsaturated lipid content in the hippocampus of a mouse model of Alzheimer's disease. Anal. Chem. **82,** 2711–2716
https://doi.org/10.1021/ac1002728

Lira EC, Goncalves DA, Parrerias-E-Silva LT, Zanon NM, Kettelhut IC, Navegantes LC (2011): Phosphodiesterase-4 inhibition reduces proteolysis and atrogenes expression in rat skeletal muscles. Muscle Nerve **44,** 371–381
https://doi.org/10.1002/mus.22066

Lopez G, Martinez R, Gallego J, Tarancon MJ, Carmona P, Fraile MV (2001): Dietary fats affect rat plasma lipoprotein secondary structure as assessed by fourier transform infrared spectroscopy. J. Nutr. **131,** 1898–1902

Mandel WJ (1995): Cardiac Arrhythmias: Their Mechanisms, Diagnosis, and Management. (3 ed.), Lippincott, Williams & Wilkins

Marsh D (1990): Lipid-protein interactions in membranes. FEBS Lett. **6,** 61–66
https://doi.org/10.1016/0014-5793(90)81288-Y

McKenna JM, Muller GW (2006): Medicinal chemistry of PDE4 inhibitors. In: Cyclic Nucleotide Phosphodiesterases in Health and Disease. (Ed. JA Beavo, SH Francis and MD Houslay), CRC Pres, New York

Mclntyre TM, Hazen SL (2010): Lipid oxidation and cardiovascular disease: Introduction to a review series circulation research. Cir. Res. **107,** 1167–1169
https://doi.org/10.1161/CIRCRESAHA.110.224618

Mika D, Leroy J, Vandecasteele G, Fischmeister R (2012): PDEs create local domains of cAMP signaling. J. Mol. Cell. Cardiol. **52,** 323–329
https://doi.org/10.1016/j.yjmcc.2011.08.016

Miller L. M, Bourassa M. W, Smith R. J. (2013): FTIR spectroscopic imaging of protein aggregation in living cells. Biochim. Biophys. Acta **1828,** 2339–2346
https://doi.org/10.1016/j.bbamem.2013.01.014

Moe KT, Wong P (2010): Current trends in diagnostic biomarkers of acute coronary syndrome. Ann. Acad. Med. Singap. **39,** 210–215

Molina CE, Leroy J, Richter W, Xie M, Scheitrum C (2012): Cyclic adenosine monophosphate phosphodiesterase type 4 protects against atrial arrhythmias. J. Am. Coll. Cardiol. **59,** 2182–2190
https://doi.org/10.1016/j.jacc.2012.01.060

Nordestgaard B (2014): Triglycerides and cardiovascular disease. Lancet **384,** 626–635
https://doi.org/10.1016/S0140-6736(14)61177-6

Ozek NS, Bal B, Sara Y, Onur R, Severcan F (2014): Structural and functional characterization of simvastatin-induced myotoxicity in different skeletal muscles. Biochim. Biophys. Acta **406,** 406–415
https://doi.org/10.1016/j.bbagen.2013.09.010

Perilli G, Saraceni C, Daniels MN, Ahmad A (2013): Diabetic ketoacidosis: a review and update. Curr. Emerg. Hosp. Med. Rep. **1,** 10–17
https://doi.org/10.1007/s40138-012-0001-3

Ramana KV, Srivastava S, Singhal SS (2014): Lipid peroxidation products in human health and disease. Oxid. Med. Cell. Longev. 162414

Rao JY, Xi L (2009): Pivotal effects of phosphodiesterase inhibitors on myocyte contractility and viability in normal and ischemic hearts. Acta Pharmacol. Sin. **30,** 1–24 https://doi.org/10.1038/aps.2008.1

Rennard SI, Schachter N, Strek M (2006): Cilomilast for COPD: results of a 6-month, placebo-controlled study of a potent, selective inhibitor of phosphodiesterase 4. Chest **1,** 56–66 https://doi.org/10.1378/chest.129.1.56

Rezvanfar MA, Ranjbar A (2010): Biochemical evidence on positive effects of rolipram a phosphodiesterase-4 inhibitor in malathion-induced toxic stress in rat blood and brain mitochondria. Pestic. Biochem. Physiol. **98,** 135–1343 https://doi.org/10.1016/j.pestbp.2010.06.001

Saberwal G, Nagaraj R (1994): Cell-lytic and antibacterial peptides that act by perturbing the barrier function of membranes: facets of their conformational features, structure-function correlations and membrane-perturbing abilities. Biochim. Biophys. Acta **1197,** 109–131 https://doi.org/10.1016/0304-4157(94)90002-7

Szczerbowska-Boruchowska M, Dumas P, Kastyak M, Chwiej J (2007): Biomolecular investigation of human substantia nigra in Parkinson's disease by synchrotron radiation Fourier transform infrared microspectroscopy. Arch. Biochem. Biophys. **459,** 241–248 https://doi.org/10.1016/j.abb.2006.12.027

Severcan F, Bozkurt O, Gurbanov R, Gorgulu G (2010): FT-IR spectroscopy in diagnosis of diabetes in rat animal model. J. Biophotonics **3,** 621–626 https://doi.org/10.1002/jbio.201000016

Severcan F, Gorgulu G, Turker S, Gorgulu ST, Guray T (2005): Rapid monitoring of diabetes-induced lipid peroxidation by Fourier transform infrared spectroscopy: evidence from rat liver microsomal membranes. Anal. Biochem. **39,** 36–40 https://doi.org/10.1016/j.ab.2005.01.011

Smyth EM, Grosser T, Wang M, Yu Y, FitzGerald GA (2009): Prostanoids in health and disease. J. Lipid Res. **50,** S423–428 https://doi.org/10.1194/jlr.R800094-JLR200

Travo A, Desplat V, Barron E, Poychicot-Coustau J, Guillon, G. Déléris I (2012): Basis of a FTIR spectroscopy methodology for automated evaluation of Akt kinase inhibitor on leukemic cell lines used as model. Anal. Bioanal. Chem. **404,** 1733–1743 https://doi.org/10.1007/s00216-012-6283-1

Turker S, Ilbay, G, Severcan M, Severcan F (2014a): Investigation of compositional, structural, and dynamical changes of pentylenetetrazol-induced seizures on a rat brain by FT-IR spectroscopy. Anal Chem **86,** 1365–1403 https://doi.org/10.1021/ac402992j

Turker S, Ilbay, G, Severcan M, Severcan F (2014b): Epileptic seizures induce structural and functional alterations on brain tissue membrane. Biochim. Biophys. Acta **1838,** 3088–3096 https://doi.org/10.1016/j.bbamem.2014.08.025

Turker-Kaya S, Mutlu O, Çelikyurt IK, Akar F, Ulak G (2016): Tianeptine, olanzapine and fluoxetine show similar restoring effects on stress induced molecular changes in mice brain: An FT-IR study Spectrochim. Acta A Mol. Biomol. Spectrosc. **161,** 178–185 https://doi.org/10.1016/j.saa.2016.02.038

Verde I, Vandecasteele G, Lezoualc'h F, Fischmeister R (1999): Characterization of the cyclic nucleotide phosphodiesterase subtypes involved in the regulation of the L-type Ca2+ current in rat ventricular myocytes. Br. J. Pharmacol. **127,** 65–74 https://doi.org/10.1038/sj.bjp.0702506

Received: November 9, 2016
Final version accepted: February 28, 2017